Articles

Pressure Response of an Organic−Inorganic Perovskite: Methylammonium Lead Bromide

I. P. Swainson,*,† M. G. Tucker,‡ D. J. Wilson,§ B. Winkler,§ and V. Milman||

Canadian Neutron Beam Centre, Station 18, Chalk River Laboratories, Chalk River, Ontario K0J 1J0, Canada, ISIS Facility, Rutherford Appleton Laboratory, Chilton, Didcot, Oxon OX11 0QX, United Kingdom, Institut für Mineralogie Abteilung Kristallographie, Johann Wolfgang Goethe−Universität, Senckenberganlage 30, D-60054 Frankfurt, Germany, and Accelrys Incorporated, 334 Science Park, Cambridge CB4 0WN, United Kingdom

Received September 11, 2006. Revised Manuscript Received February 20, 2007

The behavior of the organic−inorganic perovskite, methylammonium lead bromide, as a function of pressure was studied up to pressures slightly above 3 GPa at temperatures between ambient and ∼80 K using neutron diffraction. The sample transforms from $Pm\bar{3}m$ to $Im\bar{3}$ just below 1 GPa and amorphizes around 2.8 GPa without the cations undergoing long-range orientational ordering. The response of the orientationally ordered *Pnma* phase to pressure, which could not be accessed experimentally, was studied with density functional theory methods. The major source of volume reduction under compression is by tilting, and to a lesser extent shrinking, of the $PbBr_6$ octahedra.

Introduction

True perovskites, ABX_3, are a structure type of corner-bonded BX_6 octahedra forming a fully three-dimensionally bonded framework.[1] Organic−inorganic perovskites (OIPs) are perovskites in which the *A* cation is organic, typically an amine.[2] On cooling, OIPs undergo a variety of transitions.[3−8] These involve tilt transitions of the octahedra, and tilting is coupled in many cases to lone-pair distortions of the central atom in the octahedra and orientational ordering of the organic cations occupying the interstices between the tilted octahedra. Interactions between cation ordering and acoustic modes are responsible for incommensurate transitions in some of these compounds on cooling.[9] At low temperatures, there are a great variety of structures containing ordered organic cations seen as a function of composition, and it seems reasonable to expect a similar variety upon an increase in pressure. Methylammonium lead bromide, $MAPbBr_3$, was chosen as the material of study as MA can be relatively easily purchased or synthesized fully deuterated. $MAPbBr_3$, compared to many OIPs, has a simple ordered phase: a standard *Pnma* cell that does not involve a lone-pair distortion on Pb^{2+}.[8] At ambient pressure, this is stable below 148.35 K.[10] Onoda-Yamamuro et al. extended the boundaries of the phases of $MAPbCl_3$, $MAPbBr_3$, and $MAPbI_3$ seen at ambient pressure up to 0.2 GPa using DTA methods.[11]

The response to pressure of perovskites with even simple cations can be quite varied and has become a considerable topic of interest; e.g., in $PrAlO_3$, the proportional shrinkage of AX_{12} and BX_6 are comparable,[12] whereas in $LaCrO_3$, the contraction of the BX_6 octahedra is the main response to pressure.[13] The concept of bond valence has proved quite successful at predicting tilt systems of perovskites and the magnitude of the compression of the AX_{12} and BX_6 units.[14−16] However, bond valence is not readily calculated in systems with complex cations and hydrogen bonding, so that such

* Corresponding author. E-mail: ian.swainson@nrc.gc.ca.
† Chalk River Laboratories.
‡ Rutherford Appleton Laboratory.
§ Johann Wolfgang Goethe−Universität.
|| Accelrys.

(1) Mitchell, R. H. *Perovskites: Modern and Ancient*; Almaz Press: Thunder Bay, ON, 2002.
(2) Mitzi, D. B. *J. Chem. Soc., Dalton Trans.* **2001**, 1−12.
(3) Depmeier, W.; Möller, A. *Acta Crystallogr., Sect. B* **1980**, *36*, 803−807.
(4) Yamada, K.; Isobe, K.; Tsuyama, E.; Okuda, T.; Furukawa, Y. *Solid State Ionics* **1995**, *79*, 152−157.
(5) Yamada, K.; Isobe, K.; Okuda, T.; Furukawa, Y. *Z. Naturforsch., A: Phys. Sci.* **1994**, *49*, 258.
(6) Okuda, T.; Gotou, S.; Takahashi, T.; Terao. H.; Yamada, K. *Z. Naturforsch.* **1996**, *51*, 686.
(7) Yamada, K.; Mikawa, K.; Okuda, T.; Knight, K. *J. Chem. Soc., Dalton Trans.* **2002**, 2112−2118.
(8) Swainson, I. P.; Hammond, R. P.; Soullière, C.; Knop, O.; Massa, W. *J. Solid State Chem.* **2003**, *176*, 97−104.
(9) Swainson, I. P. *Acta Crystallogr., Sect. B* **2005**, *61*, 616−626.
(10) Knop, O.; Wasylishen, R. E.; White, M. A.; Cameron, T. S.; Van Oort, M. J. M. *Can. J. Chem.* **1990**, *68*, 412−422.
(11) Onoda-Yamamuro, N.; Yamamuro, O.; Matsuo, T.; Suga, H. *J. Phys. Chem. Solids* **1992**, *53*, 277−281.
(12) Kennedy, B. J.; Vogt, T.; Martin, C. D.; Parise, J. B.; Hriljac, J. A. *Chem. Mater.* **2002**, *14*, 2644−2648.
(13) Oikawa, K.; Kamiyama, T.; Hashimoto, T.; Shimojyo, Y.; Morii, Y. *J. Solid State Chem.* **2000**, *154*, 524−529.
(14) Lufaso, M. W.; Woodward, P. M. *Acta Crystallogr., Sect. B* **2001**, *57*, 725−738.
(15) Zhao, J.; Ross, N. L.; Angel R. J. *Acta Crystallogr., Sect. B* **2004**, *60*, 263−271.
(16) Zhao, J.; Ross, N. L.; Angel R. J. *Acta Crystallogr., Sect. B* **2006**, *62*, 431−439.

10.1021/cm0621601 CCC: $37.00
Published on Web 04/24/2007

approaches are not readily applied to this class of perovskites. X-ray powder diffraction data taken at pressure from a diamond anvil cell have been reported for tin(II) iodide OIPs containing MA and formamidinium, FA: $MASnI_3$, $FASnI_3$, and $(FA,MA)SnI_3$.[17] This same study reported $FASnI_3$ as the most compressible perovskite known. Yet the cations are more rigid objects than the octahedra in these compounds, so that it is not clear what the compression mechanism in OIPs. To examine the pressure response, we performed neutron powder diffraction on fully deuterated $MAPbBr_3$ to test whether cation ordering is coupled to tilting under pressure (as it is on cooling), because this technique is very sensitive to the ordering of D atoms, even in cages of Pb and Br. We have also performed calculations on the basis of density functional theory of the lowest-temperature phase of $MAPbBr_3$ in order to determine the detailed structural response of a fully ordered phase to pressure.

Diffraction Measurements

Neutron diffraction experiments were performed on CD_3ND_3-$PbBr_3$ using a V4 Paris-Edinburgh cell on the 90° bank of the Pearl/HiPr diffractometer located as ISIS, Chilton, Didcot, UK. An internal pressure standard of NaCl was added for room-temperature pressurization and made up ~25 vol % of the final sample. The bulk constant of NaCl is 24.7 GPa,[18] and that of $MAPbBr_3$ is greater in value. Because of its low proportion and the presence of a pressure medium, we assume that the presence of the standard does not significantly affect the pressure response of the unit cell of $MAPbBr_3$. Peaks due to the sample, NaCl, WC, and Ni are observed in the diffraction pattern that spans the range of 0.74−3.65 Å. Null-scattering TiZr encapsulated gaskets were used. For experiments at room temperature, an automated double-syringe pump was used to control pressure.

The selection of the pressure-transmitting medium was done with three factors in mind: first, it should have a glass transition at pressures higher than that of fluorinert (i.e., must be significantly higher than ~1.5 GPa); second, it should not strongly incoherently scatter, removing protonated compounds as a choice; third, it is not a strongly polar solvent. 2-Propanol-d_8 (perdeuterated isopropanol) was selected. The chemical stability of the sample in this solvent at ambient pressure was tested prior to the experiment, as more-polar solvents like water and methanol can dissolve the amine. The glass-transition pressure of protonated 2-propanol is ca. 4.2 GPa,[19] and the melting point at ambient pressure is 185 K.[20] These physical properties are expected to be only moderately affected by deuteration.

For experiments below room-temperature, pentane was used with a manual pump to adjust the pressure as the cell was cooled to 100 K using liquid nitrogen over a period of approximately 6 h. For each adjustment of pressure, the cell was heated above 200 K in order to melt the pressure medium and minimize non-hydrostatic conditions in the sample cell. The data were fitted using GSAS[21] where the NaCl standard was modeled using the Rietveld method, and the diffraction peaks of the disordered phases of $MAPbBr_3$ were modeled using the Le Bail method.[22] Fully deuterated samples were synthesized in order to reduce incoherent scattering from the amine cation. For the ambient temperature scans, the pressure was determined by fitting to the diffraction peaks of NaCl using the equation of state of Birch.[23]

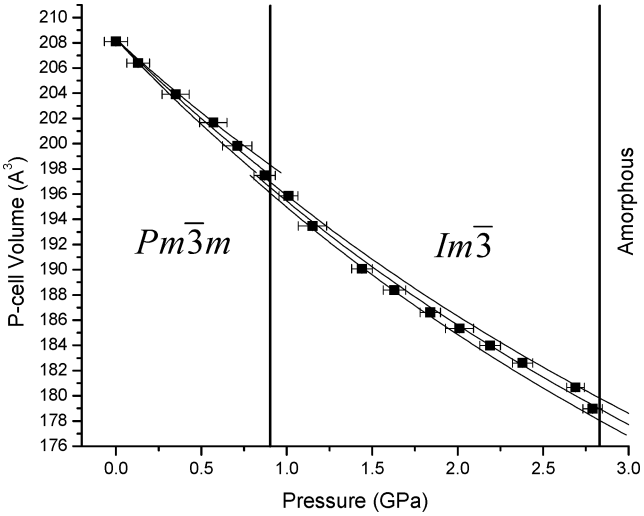

Figure 1. Volumes extracted from Le Bail fits to the Pearl data (points with esds) and the Birch−Murnaghan fits (lines; mean ± 1 esd) to the individual phases. Values are taken from Table 1.

Results

The $Pm\bar{3}m$ phase, stable under ambient conditions, was observed to transform to $Im\bar{3}$ between two observations made at 0.867(6) and 1.008(5) GPa. This phase has a doubled cell parameter with respect to that of the untilted $Pm\bar{3}m$ phase. We did not see evidence for transition to a third crystalline phase prior to amorphization in $MAPbBr_3$, which occurred at pressures above ~2.8 GPa. The amorphized sample recrystallized upon release of pressure. As no orientationally ordered phase has been observed, it appears that tilt systems that couple to volume dominate over those optimized for cation ordering.

We fitted the response of the volume of the unit cell to pressure to a Birch-Murnaghan equation of state.[18] The Birch-Murnaghan approach is strictly valid only for cubic and isotropic systems, in which there are no substructure and no internal degrees of freedom.[24] Perovskites have many non-cubic phases and all perovskites show a strong substructure consisting of the framework of octahedral, and the AX_{12} site, which in the OIPs contains the amines. Bearing in mind the above caveats, second-order Birch-Murnaghan fits to the volumes of the $Pm\bar{3}m$ and $Im\bar{3}$ phases from two different pressurization sequences are shown in Table 1 and Figure 1. The fits were performed using EosFit.[25] Only second-order fits are reported for fits to the diffraction data because of

(17) Lee, Y.; Mitzi, D. B.; Barnes, P. W.; Vogt, T. *Phys. Rev. B* **2003**, *68*, 020103-1−020103-4.
(18) Poirier J-P. *Introduction to the Physics of the Earth's Interior*, 2nd ed.; Cambridge University Press: Cambridge, U.K., 2000.
(19) Piermarini, G. J.; Block, S.; Barnett, J. D. *J. Appl. Phys.* **1973**, *44*, 5377−5382.
(20) http://www.coleparmer.com/Catalog/Msds/12090.htm.
(21) Larson, A.; Vondreele, R. *GSAS: General Structure Analysis System*; Report LAUR 86-748; Los Alamos National Laboratories: Los Alamos, NM, 1986.
(22) Le Bail, A.; Duroy, H.; Fourquet, J. L. *Mater. Res. Bull.* **1988**, *23*, 447−452.
(23) Birch, F. *J. Geophys. Res.* **1986**, *91*, 4949−4954.
(24) Angel, R. J.; Ross, N. L. *Philos. Trans. R. Soc. London, Ser. A* **1996**, *354*, 1449−1459.
(25) Angel, R. J. Equations of state. In *High-Pressure, High-Temperature Crystal Chemistry*; Hazen, R. M., Downs, R. T., Eds.; Reviews in Mineralogy and Geochemistry; Mineralogical Society of America: Chantilly, VA, 2001; Vol. 41, pp 35−60.

Table 1. Birch−Murnaghan Equations of State Fits to Pearl Diffraction Data from the Cubic Phases and the DFT-Relaxed *Pnma* Lattice (fits to the diffraction data are on the order of 2, whereas those to the DFT data are on the order of 3)

	diffraction data		DFT data		
phase	$Pm\bar{3}m$	$Im\bar{3}$	*Pnma*	*Pnma*	*Pnma*
fit	unit cell	unit cell	unit cell	AX_{12}	BX_6
V_0	208.1(1)	207.8(8)	868.8(4)	179.8(8)	37.8(2)
K_0	15.6(4)	14.1(5)	19.8 (2)	17.8 (1.1)	21.9(2.9)
K'	4	4	3.92(6)	3.96(3)	7.5(1.2)

the limited pressure range, data precision, and number of observations. When third-order fits were performed to the data of the individual phases, the goodness of fit did not improve strongly and the fitted values of V_0, K_0, and K' did not change by more than 1 esd from the values of the second-order fits. Therefore, we do not report them.

The only previous equations of state data from pressurizing OIPs were derived from fitting across all phases observed in each SnI_3-based OIP until it amorphized.[17] These fits yield values of K_0 values comparable to that seen here, but very different values of K' (fixed at 4.0 for order 2):[18,25] e.g., for $MASnI_3$, $K_0 = 12.6(7)$, $K' = 6.5(8)$ GPa; for $MA_{0.5}FA_{0.5}$-SnI_3, $K_0 = 11.5(7)$ and $K' = 10.3(9)$ GPa; and for $FASnI_3$, $K_0 = 8.0(7)$, $K' = 11.1(10)$ GPa.[17] Discontinuities are required for the $Im\bar{3} \rightarrow I4/mmm$ and $Im\bar{3} \rightarrow Immm$ transitions.[26−27] This, and the limited number of observations, may be one reason for the large values of K' reported for the SnI_3 OIPs.[17]

In an attempt to enter the orientationally ordered *Pnma* phase seen at low temperature and ambient pressures, or to discover new phases in which the cations might order, we pressurized samples to nominal pressures of 2.4 and 3.2 GPa and then cooled them to 100 K, well below the temperature at which the *Pnma* phase is entered at ambient pressure (148.35 K).[8,10] During these runs, the NaCl standard was not used in case an orientationally ordered phase was encountered, for which a structure refinement was required. However, on cooling, the sample remained in $Im\bar{3}$ at 2.4 GPa and slowly amorphized on cooling at the higher pressure. As we did not encounter any new phase, we did not perform runs on samples on cooling with a NaCl standard and we turned to other methods to examine the behavior at low temperatures and elevated pressure.

Lattice Relaxation of an Orientationally Ordered Phase using Density Functional Theory. As no orientationally ordered phase was entered experimentally, the lowest-temperature, ambient pressure *Pnma* phase was studied as a function of pressure with density functional theory (DFT) calculations performed using the CASTEP code,[28] which employs a plane wave basis set in conjunction with pseudopotentials. To approximate the effects of electron exchange and correlation, we used the PBE generalized gradient approximation (GGA) functional.[29] For computational efficiency, ultrasoft pseudopotentials[30] were chosen, which were supplied with the Materials Studio package (Accelrys, Inc.). For Pb, the 5d electrons were included in the frozen core, leaving the $6s^2$ and $6p^2$ electrons in the valence region. The accuracy of the calculation is controlled by two further parameters, namely the plane wave basis set cutoff energy and the density of k-points in the reduced wedge of the Brillouin Zone. For the former, we chose a value of 310 eV, whereas for the latter, we used a Monkhorst−Pack grid consisting of eight symmetry-unique points. Calculations were considered converged when the following four conditions were met: the change in energy/atom <5 meV residual, the forces on the atoms <0.01 eV/Å, the displacements of atoms during the geometry optimization steps <0.0005 Å, and the residual bulk stress <0.02 GPa. The calculations were performed at simulated pressures of 0, 1, 2, 3, 4, 5, and 10 GPa.

At 0 GPa, the lattice parameters of the *Pnma* cell are about 2.4% bigger in the DFT calculations than those reported at 11 K[8] and the relaxed volume is correspondingly 7.4% bigger, as is typical for such calculations. In addition to relaxations imposing *Pnma* symmetry, tests were performed in which the cell was relaxed in *P*1 in an attempt to detect possible preferred distortions. Even at 10 GPa, a search for missing symmetry suggested that *Pnma* symmetry was retained to a tolerance of better than 1×10^{-4} Å. Figure 2 shows the relaxed structures viewed down the *b*-axis at 0 and 10 GPa on a common scale.

The first coordination polyhedron around the *B*-site is the molecular anion, the BX_6 octahedron. The molecular cation and the first coordination polyhedron around the *A*-site are not identical, the former being smaller and less symmetric than the AX_{12} coordination volume, which is the underlying reason for disorder in these structures. Cell-volume contraction comes from three factors: shrinkage of the two component ions and tilting of the octahedra, which consumes AX_{12} volume. Figure 3 shows the relative importance of these components in the *Pnma* lattice. If shrinkage of the octahedra were the only phenomenon at play, then the volume of the BX_6 octahedra, unit cell and AX_{12} would all fall on the same line. Shrinkage of the $PbBr_6$ octahedron is appreciable, although tilting of these units is responsible for the majority of the volume reduction (Figure 3). The behavior of the volume of the unit cell more closely follows the behavior of AX_{12} volume than that of the BX_6 volume, showing tilting dominates (Figure 3). As the octahedron shrinks, it generally becomes slightly more regular as defined both by variability of the $B-X$ bond lengths, measured by quadratic elongation, and more obviously by the angular variance of the $X-B-X$ angles (Table 2).[31−33] Although the MA cations are very rigid, they are quite elongated in shape, which can readily be accommodated in the anisotropic AX_{12} sites created by tilting BX_6 octahedra.

Observations on Tilting in the OIPs under Pressure. For a corner-bonded network of octahedra, a tilt of one octahedron about one axis causes tilting in the opposite sense of neighboring octahedra in the plane normal to the rotation

(26) Howard, C. J.; Stokes, H. T. *Acta Crystallogr., Sect. B* **1998**, *54*, 782−789.
(27) Howard, C. J.; Stokes, H. T. *Acta Crystallogr., Sect. B* **2002**, *58*, 564−565.
(28) Segall, M. D.; Lindan, P. J. D.; Probert, M. J.; Pickard, C. J.; Hasnip, P. J.; Clark, S. J.; Payne, M. C. *J. Phys.: Condens. Matter* **2002**, *14*, 2717−2743.
(29) Perdew, J. P.; Burke, K.; Ernzerhof, M. *Phys. Rev. Lett.* **1996**, *77*, 3865−3868.
(30) Vanderbilt D. *Phys. Rev. B* **1990**, *41* 7892−7896

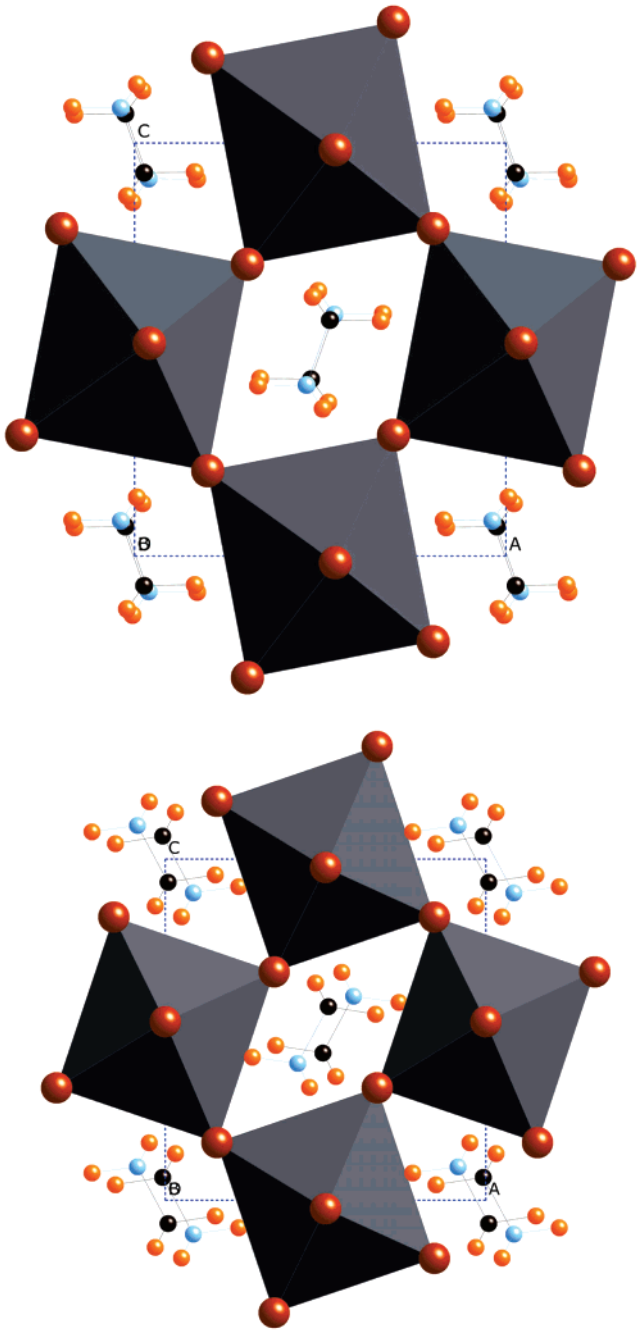

Figure 2. Plots of the *Pnma* lattice on a common scale derived from DFT relaxation at 0 and 10 GPa. The methylammonium cations (N, blue; C, black; D, orange) can be seen in the interstices between the $PbBr_{6/2}$ octahedra. Increased tilting and shrinkage of the octahedra are apparent.

(Figure 2). However, no sense of rotation is imposed on octahedron bonded above and below, which are free to rotate either in-phase or out-of-phase.[26,34−35] This choice of tilting is described by the M_3^+ and R_4^+ representations of the $Pm\bar{3}m$ lattice and can occur about all three of the pseudo-cubic axes. Tilts are often described using the Glazer symbols; e.g., the $Im\bar{3}$ structure seen in $MAPbBr_3$ and in several SnI_6 OIPs under pressure is described as $a^+a^+a^+$, representing in-phase (M_3^+) tilting of equal magnitude about all three pseudocubic axes. The additional crystalline phases reported in the SnI_6-OIPs prior to amorphization[17] are also in-phase tilt systems, derived by action of different components of the M_3^+ representation: I4/*mmm* $a^0b^+b^+$ and *Immm* $a^+b^+c^+$, where ^{0} represents no tilting and b^+ and c^+ represent different magnitudes of M_3^+ tilting about the different axes.[26−27] Because the site symmetries of the *A* cations in I4/*mmm*, $Im\bar{3}$, and *Immm* are incompatible with ordered MA or FA cations, the amorphization must also occur in the SnI_3 OIPs before long-ranged orientational ordering of the amine cations.[17]

Table 2. Geometric Parameters from the DFT Calculations of the *Pnma* Phase[a]

P (GPa)	*V* (Å^3)	QE	BAV (deg^2)	C−H (Å)	C−N (Å)	N−D (Å)	Pb−Br (Å)
0	37.9297	1.0104	36.83	1.0949	1.4912	1.0470	3.069
1	36.2633	1.0102	35.99	1.0948	1.4894	1.0468	3.023
2	35.3475	1.0079	28.00	1.0944	1.4872	1.0468	2.994
3	34.2626	1.0080	28.26	1.0937	1.4850	1.0465	2.963
4	33.7198	1.0064	22.65	1.0928	1.4839	1.0472	2.945
5	33.4521	1.0081	28.77	1.0924	1.4818	1.0467	2.955
10	30.5901	1.0054	20.02	1.0897	1.4735	1.0445	2.849

[a] *V* is the volume of a BX_6 octahedron, QE is the quadratic elongation, and BAV is the bond angular variance;[28−30] the bond lengths of the components are given in the right-hand columns.

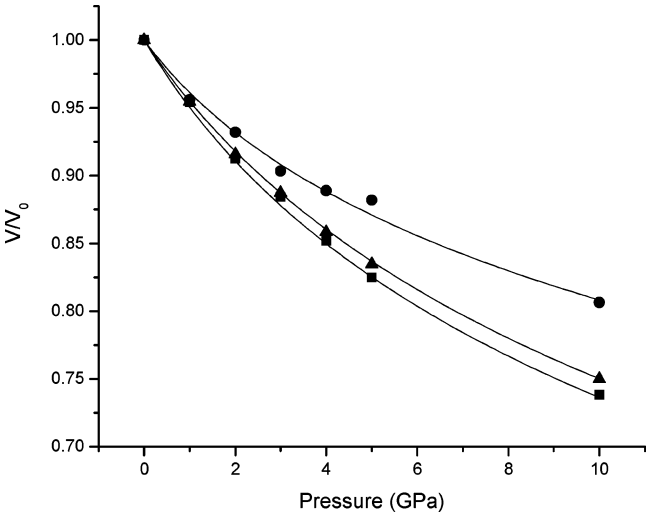

Figure 3. V/V_0 plots of the unit cell, AX_{12} and BX_6 volumes of the DFT-relaxed *Pnma* lattice. The behavior of the normalized unit-cell volume (triangles) is closer to that of the normalized AX_{12} volume (squares), determined by tilting of octahedra, than to the normalized volume of the BX_6 octahedra (circles).

The *Pnma* phase observed at low-temperature corresponds to the tilt system $a^+b^-b^-$, in which there is a component of in-phase tilting about one axis and where the b^- symbol represents a different magnitude of out-of-phase (described by R_4^+) tilting about the other two axes. Figure 4 shows the structure looking down the *b*-axis, about which the in-phase M_3^+ component of tilt, the largest component of tilt, occurs. The smaller R_4^+ tilts take place about <101> axes lying in the plane. The M_3^+ and R_4^+ components of tilt, $\vartheta_{M_3^+}$ and $\vartheta_{R_4^+}$, were retrieved as a function of pressure using the geometrical analysis method of Thomas[36] (Figure 4). Although total tilting increases with pressure, it does so only by increase of the in-phase component, $\vartheta_{M_3^+}$, which is also the style of tilting that dominates the phases observed at high temperature.

Conclusions

The diversity of structures seen upon cooling in the organic−inorganic perovskites does not appear to be present

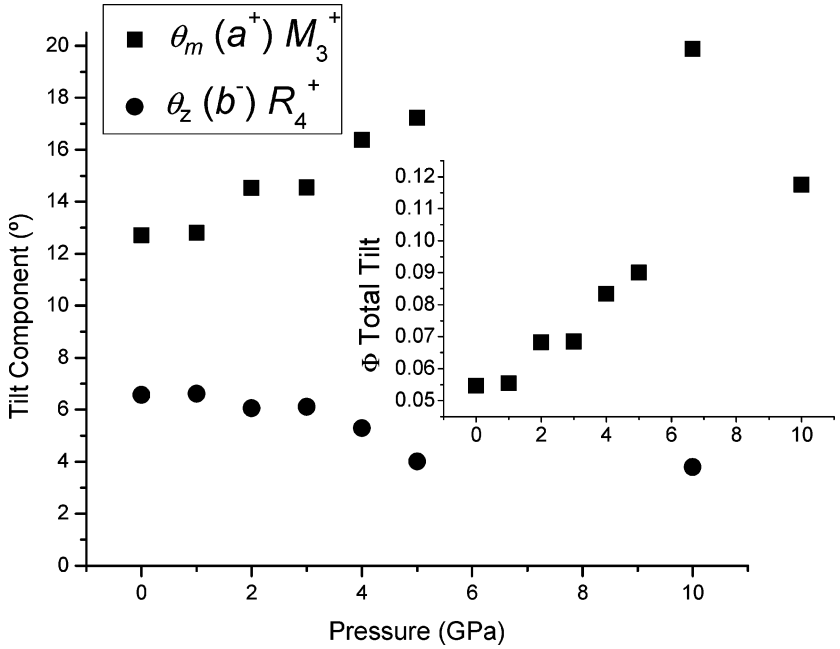

Figure 4. M_3^+ (squares) and R_4^+ (circles) tilt components as a function of pressure in the DFT-relaxed *Pnma* lattice. Inset: Total tilting magnitude, Φ, as defined by Thomas.[36] Total tilting increases with volume almost exclusively because of an increase in the M_3^+ component.

upon compression. $MAPbBr_3$ amorphized at relatively low pressures, as was reported in the case of related Sn(II) salts. In the latter study, the pressure medium of fluorinert froze at ca. 1.5 GPa, whereas 2-propanol does not freeze in this pressure range. Therefore, deviatoric stresses due to the pressure medium are an unlikely trigger for the observed pressure-induced amorphization in these OIPs at ambient temperature. In the OIPs studied to present, all amorphize prior to the organic cations undergoing long-range orientational ordering. One open question for future research is the effect amorphization has on the initially dynamic disorder of the cations in the crystalline forms. The $Pm\bar{3}m \rightarrow Im\bar{3}$ transition is the first observed in all studied OIPs, regardless of the organic or inorganic sublattices. This strongly implies that the energy gain for orientational ordering is low and that volume reduction is the main driving force for transitions of these compounds under pressure. All the phases observed under pressure in the OIPs studied to date are dominated by M_3^+ tilt components.

CM0621601

(31) Balić Žunić, T.; Vicković, I. *J. Appl. Crystallogr.* **1996**, *29*, 305−306.
(32) Robinson, K.; Gibbs, G. V.; Ribbe, P. H. *Science* **1971**, *172*, *567*−570.
(33) Finger, L. W. *VOLCAL*; Geophysical Laboratory, Carnegie Institute of Washington: Washington, D.C., 1971.
(34) Glazer, A. M, *Acta Crystallogr., Sect. B* **1972**, *28*, 3384−3392.
(35) Glazer, A. M. *Acta Crystallogr., Sect. A* **1975**, *31*, 756−762.
(36) Thomas, N. W. *Acta Crystallogr., Sect. B* **1996**, *52*, 16−31.